3 Multi-detector analysis

3.1 Coincidence search

This is the simplest multi-detector analysis that can be done, and the required information are just the amplitude and time of arrival of the events along with their error statistics and the detection efficiency as a function of signal amplitude. The choice of amplitude thresholds and time windows are a consequence of subjective statements of what false dismissal and false alarm rate are considered 'reasonable'.

A claim about a gw event can only be a statement on the (un)certainty of the detection. Results are expressed giving probabilities at different confidence levels. As the detector characteristics are not stationary, false alarm estimates with Poisson point models are to be integrated with shifts/shuffles of the real data. Limits of both methods are discussed.

3.1.1 Overview of the method

The more basic multi detector analysis that could be devised is just a data reduction by point-coincidence search. It applies –of course– to any kind of non-periodic signal, provided that all detectors used the same templates for $h(t;a)$.

The outline of the fundamental tasks to be performed in order to achieve a result –either an upper limit or a detection claim– is the following:

a) To define what is meant for coincidence, taking care of concurrent requests about false alarm and false dismissal probability.
b) To provide a method for the identification of the events in coincidence (easy?!).
c) To provide an estimate of the expected background.
d) To set up a test statistic, and to assign probabilities to different hypothesis on the value of the physical observable.

Let us assume that, for the kth among M detectors constituting the observatory, the list of arrival times of the events (regardless to the amplitude) can be modeled by a Poisson point process $\mathbf{t}^{(k)} = \left\{ t_i^{(k)} \in [0, T_{obs}] \right\}_{i=1,2,\ldots}$, where T_{obs} is the total time of observation, and the operation was smooth and homogeneous for the whole interval $[0, T_{obs}]$. We define tentatively an M-fold coincidence in a window t_w the process

$$\mathbf{c} = \left\{ c_n = \left(t_{i_{n,1}}^{(1)}, t_{i_{n,2}}^{(2)}, \ldots, t_{i_{n,M}}^{(M)} \right) \middle| t_{i_{n,1}}^{(m)} \in \mathbf{t}^{(m)} \forall h,k : \left| t_{i_{n,h}}^{(h)} - t_{i_{n,k}}^{(k)} \right| < 2t_w \right\}_{n=1,2,\ldots} \qquad (3.1)$$

The fact that it is a multivariate RV is not relevant, as we can later apply any single-value estimator (like the weighted mean) to the Mtuple c_i to obtain a more conventional Poisson point series representing the best estimate for the time of arrival of the gw events (and similarly for the event amplitude).

Even if there is no real signal in the event a list, false alarms take place by chance when performing a coincidence search. In the geometrical interpretation for M=2 given in Figure 21*c*, black dots represent the joint process $\underset{k}{\otimes} \mathbf{t}^{(k)}$ and false alarms is the subset of them falling into the *fiducial volume* (depicted as a gray tube) determined by the window aperture $2t_w$ trough (3.1). As such, they are proportional to the density of dots in the space of Mtuples, that is to the product of event rates in the single detector. We shall discuss extensively the topic of false alarms in 3.1.3.

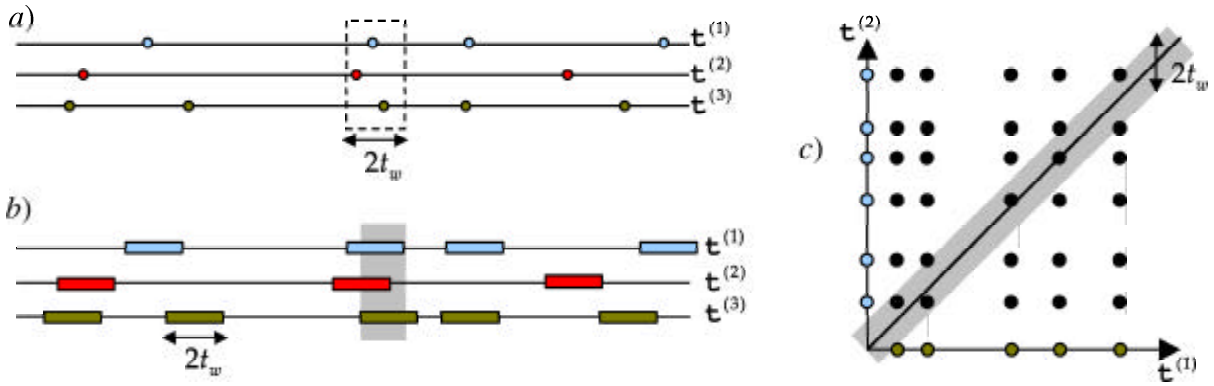

Figure 21 – Three different ways to picture (3.1): *a)* when plotted on the same axis, the times of arrival fall within a time span of $2t_w$; *b)* the uncertainty boxes of width $2t_w$ drawn around each ToA's overlap; *c)* the distance along each axis of the Mtuple of ToA's from the line $t^{(1)} = t^{(2)} = \ldots = t^{(M)}$ is less than t_w

Efficiency is just the complementary of false dismissal, i.e. the probability of missing some events that nominally should be caught by the observatory, and is conjugate to respect to false alarms. The balance between them is decided setting aperture of the time coincidence window. Efficiency becomes important when it is sensibly less than 1. In this case all resulting gw rates (either measures or upper limits) have to include a correction given by the inverse of the efficiency to become absolute counts of the incoming gw.

The efficiency is given by the joint pdf of time of arrival measurement for a real event (which is of course always centered on the bisector), integrated over the fiducial volume. You may notice that a better definition of coincidence exists which minimizes the false alarm keeping constant the efficiency. Let us assume that we know an absolute trigger time t_0, and we want to test the detection of a compatible gw event in the set of *M*tuples $\underset{k}{\otimes}\mathbf{t}^{(k)}$. The condition that define coincidence in case of a precise external trigger collapse in $\left|t^{(h)} - t_0\right| < 2t_w \quad \forall k = 1,\ldots,M$, which defines a M-dimensional hypercube centered on the bisector at coordinate t_0, and $\left|t^{(h)} - t^{(k)}\right| < 2t_w$ It is clear that better choices exists for the shape of the fiducial volume. The best solution –as you can easily figure out– is the isodensity contour of the joint pdf that include a probability volume equal to the desired efficiency (see Figure 22). However, the difference with respect to taking a box is not immense. If the pdf is not perfectly known, or if we can tolerate an overestimate of a factor two of the false dismissal (as when we just need a choice for t_w that makes it negligible) a boxed volume is perfectly acceptable first-order solution.

This kind of reasoning can be applied (with appropriate refinements) also to the original definition of coincidence, whose fiducial volume is obtained by translation of the hypercube

Figure 22 – A two-dimensional Gaussian density function clipped in a circular domain has a smaller radius than in the case of square domain (with equal volume integral).

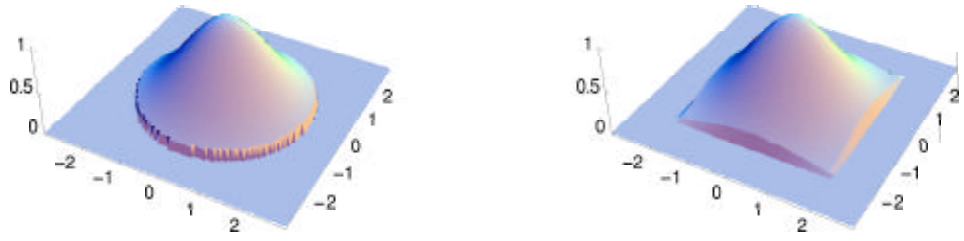

(or whatever we chose for the triggered coincidence case) along the bisector because of ignorance of the absolute ToA of the event.

3.1.2 Remarks on detection efficiency

There are three main sources of false dismissal (i.e. low efficiency).

a) *Timing errors*: the more we close a coincidence window, the more we are like to miss a coincidence, because of the natural spread of the estimated time of arrival around the true one. The false dismissal is given by the two-tailed probability distribution of the time of arrival error.

b) *Amplitude selection*: If we ask for the number of events with amplitude greater than a certain threshold A_{th}, we apparently miss half of the events whose *true* amplitude was at the threshold edge, because the measured amplitude is lowered by the additive amplitude noise. Signals with amplitude greater than A_{th} have less chance to be skipped, while signals with lower amplitude can jump above the threshold. There is a subtlety linked to this point. Let $f_a(a;A)$ be the (additive) amplitude noise pdf for signals with amplitude A[12], $f(A)$ the *amplitude spectrum* of the incoming gw signals. The estimate $\hat{F}(A)$ of the *cumulative amplitude spectrum* $F(A)$ obtained by amplitude selection is

$$\hat{F}(A_{th}) = \int_{A_{th}}^{\infty} dA \int_{0}^{\infty} da\, f_a(A;a) f(a) \qquad (3.2)$$

We can often assume that $f_a(A;a) \approx f_a(A-a)$. In such case (3.2) becomes

$$\hat{F}(A_{th}) \approx f_a * F(a) \qquad (3.3)$$

The measured spectrum is a smeared version of the real one. Therefore, it is not so obvious that we are *missing* events. If the gw events are peaked at a particular amplitude, $f(A) \approx \delta(A - A_0)$, then $\hat{F}(A_{th}) \approx 1 - F_a(A_{th})$, i.e. $\hat{F}(A_{th}) < F(A_{th})$ for $A_{th} < A_0$. However this kind of distribution seems rather the product of an artificial source, and could not have a counterpart in the real world. Instead it is more reasonable that $F(A_{th})$ is a decreasing function of the amplitude (for example). In this case the net effect of the noise is to populate the distribution above the threshold with events of lower amplitude.

c) *Dead time*: apart from the bare non-operative time due to maintenance of the detector, it should be kept in mind that –due to the specific search algorithm that was applied to the data (see 1.3.2)– the detector is insensitive for a few multiples of the Wiener time around each detected event, including those generated by environmental disturbances, and removed by χ^2 test or anticoincidence with auxiliary probes. Even when the event passes the χ^2 test, and there is no other clue of a local source for it, but it was not in coincidence with an event of other simultaneously operating detectors we should just say that *if* there were another event much smaller in amplitude nearby, than it would be shadowed by the detected one. The hypothesis of an event much *larger* in amplitude can however be ruled out. Therefore, the efficiency is also a function of the amplitude.

---

[12] For instance, if the noise is Gaussian $f_a(A;a) = \dfrac{e^{\frac{(A-a)}{2\sigma^2}} + e^{\frac{(A+a)}{2\sigma^2}}}{\sqrt{2\pi}\sigma} \approx \dfrac{1}{\sqrt{2\pi}\sigma} e^{\frac{(A-a)}{2\sigma^2}}$.

A promising method to determine the efficiency of detection is through careful use of the results of software signal presence analysis (as we report in 4.3.3).

3.1.3 Theoretical models for false alarms

Let λ^k be the rate of events in the *k*th detector, λ_b the rate of coincidences in presence of pure background uncorrelated noise[13]. We maintain that

$$\lambda_b = M(2t_w)^{M-1}\prod_{i=1}^{M}\lambda^{(k)} \qquad (3.4)$$

To begin the proof of this, we observe that for every given set $\{t^{(1)},t^{(2)},\ldots,t^{(M)}\}$ of times of arrival, the corresponding probability density $P(t_i^{(1)},t_i^{(2)},\ldots,t_i^{(M)})$ that the set of are a certain *M*tuple stay the same no matter how we permute the entries. So it is not restricting to consider only the case of ordered time coordinates $t_i^{(1)} < t_i^{(2)} < \ldots < t_i^{(M)}$, as long as we correct our following calculation by a factor $M!$.

Let us consider the measure of a small box in the canonical space of all possible outcome coincidences, with coordinates bounded between $t^{(k)}$ and $t^{(k)}+dt^{(k)}$ for each *k*. The probability of having an *M*fold coincidence inside this infinitesimal box is $dP(M)=\prod_{k=1}^{M}\lambda^{(k)}dt^{(k)}$, and by integrating this expression for all values of the time coordinates allowed by the ordering condition we find the number of coincidences in a finite window t_w in the observation time T_{obs}:

$$T_{obs}\lambda_b = \int_0^{T_{obs}} dt^{(1)} \int_{t^{(1)}}^{t^{(1)}+2t_w} dt^{(2)} \cdots \int_{t^{(M-1)}}^{t^{(1)}+2t_w} dt^{(M)} \prod_{k=1}^{M}\lambda^{(k)} = \qquad (3.5)$$

$$= T_{obs}\prod_{k=1}^{M}\lambda^{(k)} \int_0^{2t_w} dt^{(2)} \cdots \int_{t^{(M-2)}}^{2t_w} dt^{(M-1)} \int_{t^{(M-1)}}^{2t_w} dt^{(M)} = T_{obs}\frac{(2t_W)^{M-1}}{(M-1)!}$$

Restoring the factor $M!$ to take into account reordering of the times of arrivals, we obtain the desired result.

Equation (3.4) holds in the limit of a time span small enough that we can disregard the unavoidable non homogeneous behavior of the detector parameters (event rate, which is in turn affected by sensitivity, and so on). The natural extension of this formula is

$$\lambda_b(t) = M(2t_w)^{M-1}\prod_{i=1}^{M}\lambda^{(k)}(t) \quad \Leftrightarrow \quad \overline{\lambda}_b = M(2t_w)^{M-1}\int_{t=0}^{T} dt\prod_{i=1}^{M}\lambda^{(k)}(t) \qquad (3.6)$$

Let us comment equation (3.6). If we multiply it by the observation time, on the left side we obtain the number of found coincidences in the observation time, $\mathbf{N}_b = \overline{\lambda}_b T_{obs}$. Under the very general assumption that the events are uncorrelated and rare (i.e. negligible probability of double coincidence) the probability distribution of $\mathbf{N}_b$ is Poisson even if the detector is not

---

[13] We don't distinguish between the background event rate and the measured rate for the single detector, as they coincide first order. Should the rate of coincidences be found to be much greater than the estimated background and in particular not negligible with respect to λ^k, than we shall start all over again but subtracting the previously found coincidences before computing the background, getting a slightly smaller value for λ_b. Further second-order decrease of the expected accidental coincidences and increase of our confidence of detection can be achieved in the same way, recursively, until convergence.

stationary[14]. On the right side the operations of integral and product can be switched only if the processes $\{\lambda^{(k)}(t)\}_{k=1,\ldots,M}$ are uncorrelated[15]. If this is the case, then (3.6) reduces to

$$\mathbf{N}_b = \overline{\lambda}_b T_{obs} = M\left(\frac{2t_w}{T_{obs}}\right)^{M-1} \prod_{i=1}^{M} T_{obs}\overline{\lambda}^{(k)} = M\left(\frac{2t_w}{T_{obs}}\right)^{M-1} \prod_{i=1}^{M} \overline{\mathbf{N}}_b^{(k)} \qquad (3.7)$$

This sounds a big improvement, as now the RV's on both sides are just pure counts.

If the assumptions on $\{\lambda^{(k)}(t)\}_{k=1,\ldots,M}$ cannot be taken as proved *a priori*, then the effort needed for a direct test of them is almost equivalent to applying (3.6) directly[16]. In the next section we shall show how this can be practically implemented.

We shall conclude this section trying to show how these results change in case of variable time windows. It is in fact obvious that the window choice should be related to the density function of the timing error. The latter is specific to each detector and each event, as it depends on the autocorrelation function of the noise and –in general– on SNR.

In the following we are assuming that all events of a detector have the same timing error distribution, but allow for different detectors having different timing errors. The window half-length t_w used above can be defined imposing that the measured time of arrival of a gw is contained within a time span of length $2t_w$ centered on its (true) value with a certain CL. In a more general case, we deal with the set $\{t_w^{(k)}\}_{k=1,..,M}$ of windows half-length. A naïve extension of (3.1) is

$$\mathbf{c} = \left\{\left(t_i'^{(1)}, t_i'^{(2)}, \ldots, t_i'^{(M)}\right) \middle| \forall h,k : \left|t_i'^{(h)} - t_i'^{(k)}\right| < t_w^{(h)} + t_w^{(h)}\right\}_{i=1,2,\ldots} \qquad (3.8)$$

(see Figure 23).

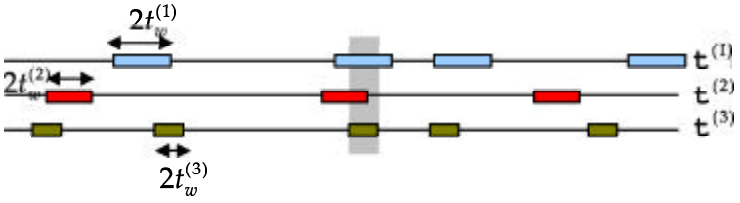

Figure 23 – Pictorial representation of (3.8)

Let study the false dismissal and the false alarm probability by interpreting (3.8) from a geometrical point of view. It can be shown that the formulas which predict the false alarm probability hold also the in case the *timing errors in the M detectors differ* but are *the same for every event* of the same detector, at the sole condition that in place of the factor $M(2t_w)^{M-1}$ we substitute

$$M(2t_w)^{M-1} \quad \leftrightarrow \quad \sum_{k=1}^{M} \prod_{h \neq k} 2t_w^{(h)} \qquad (3.9)$$

---

[14] This statement holds because the formula (3.6) for $\lambda_c(t)$ is exact as *instantaneous* rate predictor, and because linear operations (like integrals) on Poisson RV give as a result a Poisson RV.

[15] It could be said indeed that this is the *definition* of uncorrelated functions.

[16] An hybrid solution is to check that the two approaches give identical results on a couple of detectors, and then, if it is the case, use (3.7) for the case M>2.

To figure out how things are going, the reader should refer to Figure 24, where the cases M=2 and M=3 are represented. The fiducial volume is the product of the tube along the bisector and the length of the tube. The first is given by the projection of (half) the M-1 dimensional surface of the hyper-box in the plane orthogonal to the bisector, which mathematically corresponds to a multiplication of the area of each hyper-face by $1/\sqrt{n}$ (which is the common value of all the three components of the unitary vector pointing along the bisector). The second is the common observation time of the M detectors divided by the same factor. The two factors cancels out in the product, and this gives the announced result.

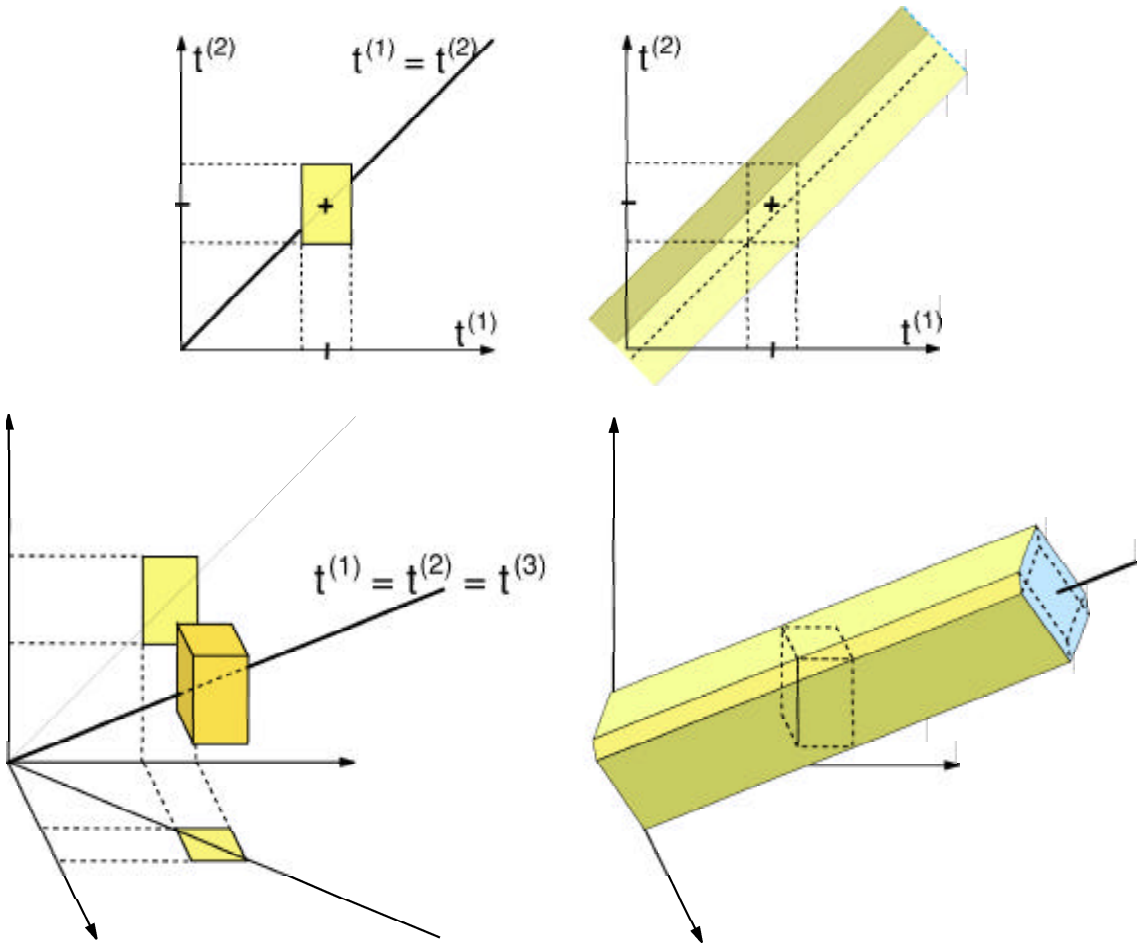

Figure 24. Geometrical interpretation of the meaning of false dismissal and false alarm, with two (*top*) and three (*bottom*) detectors. The locus of equal time coordinates is the bisector (drawn in bold black). The fiducial volume corresponding to a claim of coincidence with an external trigger is shown on the left. Without any previous notion of the time of arrival, the volume develops along the bisector.

3.1.4 False alarms estimators from the data

There are many ways we can estimate the background coincidence rate without making assumptions about the correlation of the detector noise. Here there are a few examples.

1. From a non-homogeneous Poisson model:

$$\lambda_b = \frac{\overline{n}}{T_{obs}} = T_{obs}^{-1} M \sum_i \left(\frac{2t_w}{\Delta T_i} \right)^{M-1} \prod_{k=1}^{M} n_i^{(k)}; \quad \sum_i \Delta T_i = T_{obs}$$

2. Using rigid time shifts: the time series are each other offset by constant time delays. For each time delay, a coincidence search is performed. This is repeated for a number of times enough to get statistically significant results, with time offset from 0 up to T_{max} in steps equal to T_{min}.

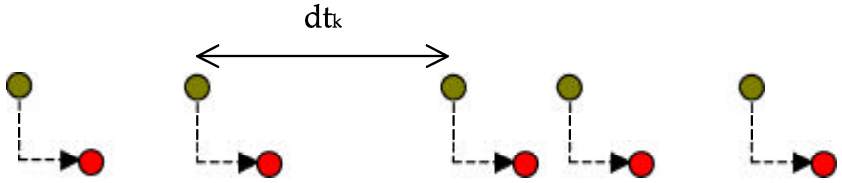

   - the statistics of delay times dt_k among events of a single detector is not changed
   - the "instantaneous" mean rate changes only on timescales up to T_{max}
   - The number of independent statistical samples is: $N = (2\ T_{max} / T_{min})^{M-1}$ with $T_{min} > \Delta t$, so that, with M=2 and N=3000, T_{max} is already about one hour.

3. Time shuffling: as 2, but with random choice of the offset from 0 to T_{max} independently for each event.

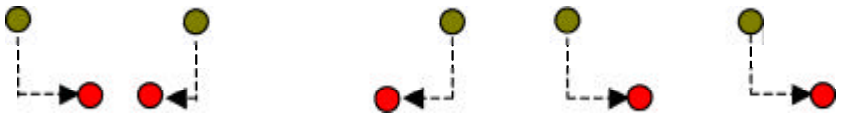

   - Statistics of dt_k changes for values of dt_k less than T_{max}
   - The instantaneous mean rate the instantaneous mean rate changes (more or less, depending on how much homogeneous was the random process) up to times long as T_{max}
   - Not a wider statistics

4. Window length dependence

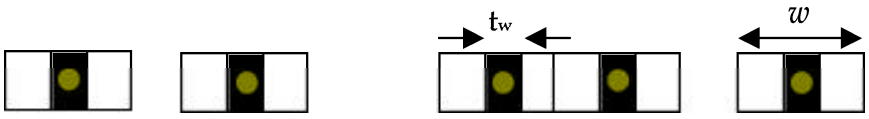

Using time windows w more and more long, excluding at zero delay a window of length t_w, and counting coincidences, we should find out the following behavior

$$\overline{n}_c(w) \propto \left[\frac{2(w - t_w)}{T_{obs}} \right]^{M-1}$$

which could be extrapolated back to w=2t$_w$.

- This method doesn't change the statistics of dt$_k$
- Extrapolation could be biased if it is based on values of w greater than characteristics times of instabilities.

We shall proceed with a few details on method 1, just because it was the technique applied to the data exchanged for the recently published IGEC paper [24] (included in the appendix as part of this work).

The starting point of this method is the estimate of the instantaneous rate of events in the kth detector $\lambda^{(k)}(t)$. To perform this task we use a sort of moving average on the time delay vs. time plot. In practice, we measure the delay Δt_i relative to consecutive groups of m events, with m chosen about 10 to reduce statistical (counting) errors to about 30%. The mean rate of events in the interval Δt_i is $\lambda_i \approx \frac{m}{\Delta t_i}$.

The list $\{(\lambda_i, \Delta t_i) \mid i = 1,2,...\}$ is then projected into a frequency histogram of the values taken by λ, weighted with the time length Δt_i of the interval within which that value was measured (basically, the histogram has binned values of λ on the x-axis, and corresponding observation time on y-axis). This histogram is eventually renormalized to get an estimator of the density function $f(\lambda)$.

In Figure 25 you can get in a shot an idea of the actual performance of this procedure in a bench test simulation.

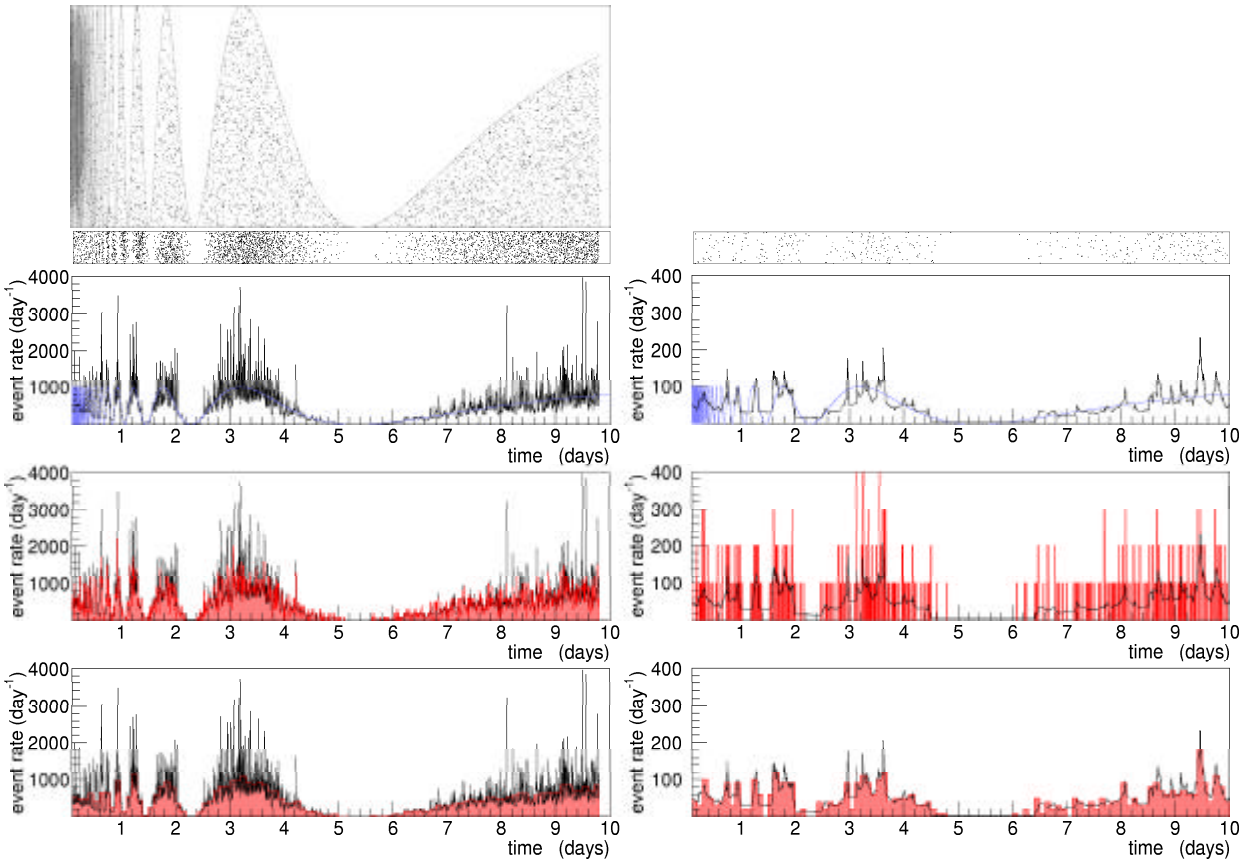

Figure 25 – (top) Graphical representation of a simple Monte Carlo simulation of a variable rate Poisson point process, modulated by the function $\sin(1/t)$. (*a*) Estimate of istantaneous rate by a constant count binning as described inthe text compared with the original rate (*blue curve*). (*b,c*) The previous estimate (*in balck*) is compared with a constant time binning, with two different choices of the bin duration differing of one order of magnitude.

In ref. [24] the empirical density function of single detectors $f^{(k)}(\lambda)$, computed as just explained, have been combined to give the density function of accidental coincidence rate $f(\lambda^c)$, which is a time independent way to represent the sensitivity of the observatory (given that the characteristics of the observatory itself do not change on average, i.e. the system is ergodic in the time span of one or two years). To go from $\{f^{(k)}(\lambda)\}$ to $f(\lambda^c)$, for each detector k we compose a statistic sample $\{\lambda_i^{(k)} | i = 1,2,...N\}$ with N~10^3, whose statistics is described by the density function $f^{(k)}(\lambda)$ (the procedure to extract such sample is straightforward, it is a standard Monte Carlo method). Next we build the set $\left\{\lambda_i^c = M(2\Delta t)^{M-1}\prod_k \lambda_i^{(k)} | i = 1,2,...N\right\}$, which – projected and normalized – gives $f(\lambda^c)$.

The results are plotted in Fig. 2 of ref. [24]. In the plot, for a given sample configuration of the observatory (that is a couple, triple or quadruple of detectors), we select the fraction of the common observation time during which the amplitude thresholds for event search were below a suitable value, say $H_{th}=3\cdot10^{-21}$ Hz^{-1} for the couple of detector ALLEGRO-AURIGA. The sample couple, triple or quadruple is chosen looking for a low threshold level, while keeping the observation time reasonably high.

For each threshold, on the x-axis the data are restricted to periods during which the detector was operating with sensitivity better than that threshold. From these subsets of the data (one for each detector) we derive the pdf $f(\lambda^c)$, as outlined above, and then we extract and plot its mean, and the mean increased by one standard deviation.

Apart from numerical inaccuracies in the computations, the mean $E\{\lambda_i^c\}$ computed this way should be exactly equivalent to that computed with the usual theoretic formula $M(2\Delta t)^{M-1}\prod_k E\{\lambda_i^{(k)}\}$.

On the other hand, the standard deviation of $f(\lambda^c)$ represents a measure of the *instantaneous* fluctuation in the accidental rate, due to non-stationary behavior of $\lambda(t)$. The statistical uncertainty in the estimates for the number of accidental coincidences expected in the average by chance in a period of T_{obs} is proportional to T_{obs}^{-1}. Compared to the predicted instantaneous fluctuation of $f(\lambda^c)$ in Fig. 2 of ref. [24], the fluctuation around the predicted mean number of accidentals for a sample period of T_{obs} ~1.5 years was about one order of magnitude less at low thresholds.

3.1.5 Detection claims and upper limits

Let us suppose that in some way we can estimate the number of expected background coincidences $\mathbf{N}_b$. Let λ_{GW} be the unknown mean rate of gw events produced by random (and rare) sources: it is natural to model this point process with a Poisson statistics. The number of coincidences $\mathbf{N}_c$ counted in a typical experiment over a time T_{obs} is therefore a Poisson RV with mean $\bar{\mathbf{N}}_c = (\lambda_b + \lambda_{GW})T_{obs}$. The probability that the outcome of the experiment –i.e. the counted coincidences– is less or equal to the observed one is the quantity

$$d = \sum_{k \le n_c} P(\mathbf{N}_b + T \cdot \lambda_{GW}) \qquad (3.10)$$

The most like λ_{GW} supported by the observations is obtained for d =0.5 and it can take positive as well as negative values in absence of g.w. signals. This should not be of any worry, because it simply means that there were fewer coincidences than what averagely expected. To avoid negative numbers, and to be more conservative in the results, a value lower than 0.5 is often used for d, after the check of consistency of $\lambda_{GW}(0.5)$ with zero. We shall say that the number of found coincidences n_c *"agrees with (1-d) confidence level (CL) with a rate at most* $\lambda_{GW}(d)$*"*, or *"* λ_{GW} *is the upper limit at (1-d) CL"* if λ_{GW} is the solution of (3.10) for any d<0.5. The frequentist interpretation of this statement is that if the true value of λ_{GW} were really $\lambda_{GW}(d)$, and $\lambda_{GW}(0.5)$ is an underestimate due to a fluctuation of the Poisson RV n_c, then only one time over 1/d a repetition of the experiment would reproduce such (or worse) result. Of course, this doesn't mean that the rate $\lambda_{GW}(d)$ has any meaning at all (by definition, it is an *unlike* optimist expectation).

It may seem strange that one can talk about a rate of gw before even one is detected. In fact, as far as we have only negative results, we could only say that in the specific time span when the detectors were operating no events were observed above a certain threshold (and allowing for a non null false dismissal!). A more general result involves some theoretical assumptions, for instance that there is a set of sources of gravitational waves we can model as a stationary random (i.e. Poisson) process. It is on the firing rate of these hypothetic sources that we are putting upper limits.

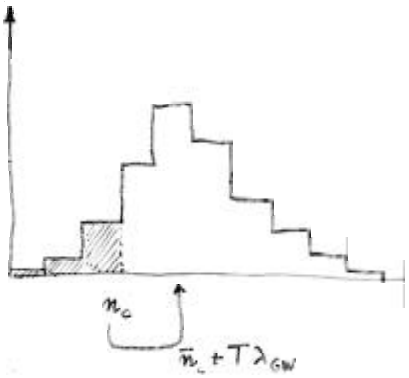

Figure 26. Interpretation of confidence level. If the true value of the rate of gravitational waves is λ_{GW}, then the probability that n_c or a lower value is obtained as the outcome of a similar experiment is given by the area *d*. (*in gray*)

3.2 Validation of results

When timing errors are sufficiently small, it become feasible to test consistency of lap times, assuming light speed propagation of the gw wave, and eventually this leads to source location.

Amplitude consistency should be tested as well, along with a refinement of χ^2 test on signal template as provided by each individual single-detector data analysis. The power of the method and the sensitivity with respect to signal template is discussed.

3.2.1 Source location

A single detector claim consists basically on the sole information about the time of arrival, while the amplitude technically is only a lower limit for the true amplitude, as we do not know the polarization angle of the incoming wave, nor the direction of the source. We can perhaps just exclude a narrow bent on a great circle where the directional sensitivity of the detector is at minimum.

The first real source location capability is provided by a couple of detectors. As the presently working detectors in IGEC are oriented parallel each other, we shall avoid complicated antenna pattern calculations restricting to this case from now on. The delay of the ToA of the wave front at the sites of the two detectors is

Figure 28 – Comprehension schetch for Eq. (3.11)

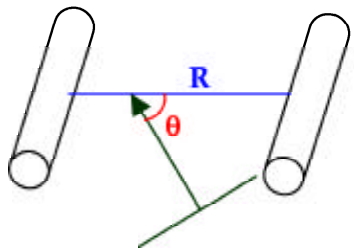

$$\Delta t = \frac{R}{c}\cos\theta \qquad (3.11)$$

with R being the distance between the two sites measured along the linear path of the gw, *c* the speed of light.

If the only contribution to timing errors is the phase error (see 1.3.3), then (3.11) represent a rather thin circle on the sky, with angular aperture given by

Figure 27 – Front and rear view of the surface map of the most likely directions in the sky for a sample choice of the phases (i.e. the times of arrival) of an event in coincidence between the three detectors AURIGA, NAUTILUS and EXPLORER. The two axis orrespond to the couples of detectors AURIGA-EXPLORER and AURIGA-NAUTILUS. Darker colors represent higher probability. The patten were computed for a detection with equal sensitivity in all detectors and SNR=5. The total area covered by the darker spots is ~2% of the sky.

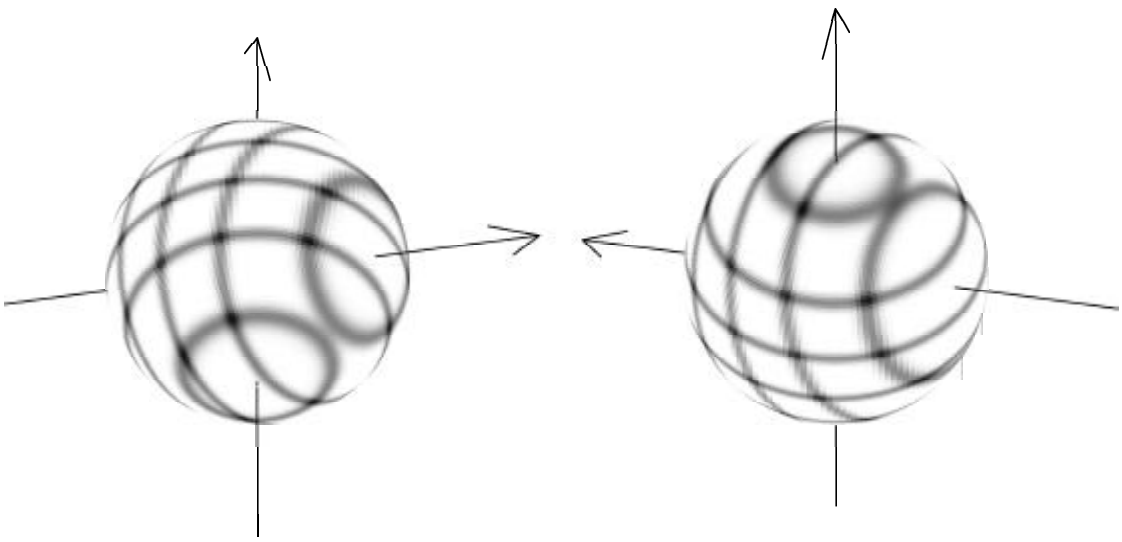

$\Delta(\cos\theta) \approx \frac{c}{R}\sigma_\phi$. Because of the peak error, other circles are allowed in a discrete set $\{\theta_k\}$, creating a striped pattern with an angular interval between each stripe given by $\cos\theta_{k+1} - \cos\theta_k \approx \frac{c}{R}\frac{\sigma_k}{\omega_0}$.

A third detector introduces a second independent time delay and a second set of stripes, which intersect the previous at a discrete set of narrow spots. [33]

Eventually, with more detectors, there is no direction consistent with the time of arrivals, and this provides a powerful method to reject the coincidence, which depends only on absolute timing calibration of the event search and time tag at each detector.

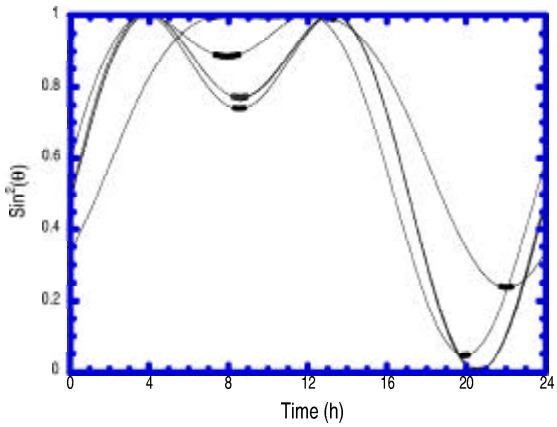

Figure 29 – The directional sensitivity of a bar detector changes within 24 hours due to Earth rotation, as it is proportional the value of the factor $\sin^2\theta$, where θ is the angle between the bar axis and the incoming gw wave direction. Because the detectors in the IGEC are almost parallel [29], the patterns are rather similar, which maximizes the detection efficency. This example shows the modulating pattern in the case of the Galactic center.

3.2.2 Likelihood test

The likelihood test in a single detector is devoted to discriminate between burst excitations of the bar and other spurious signals. Even in this way, background mechanical noise and thermal fluctuation produce a lot of events indistinguishable from a gravitational one, so that we can only put limits on the average rate of astrophysical GW bursts.

The next logical step is to use a similar technique in the context of an array of detectors to discriminate between GW bursts and *any* other signal. In fact, it was demonstrated that 6 equal optimally oriented GW detectors are needed to fully characterize the incoming GW properties (direction and polarization). A smaller number of detectors N_d, through it doesn't constitute an isotropic observatory nor is sensitive to all polarization, anyway will be able to perform a coincidence analysis capable of greatly reduce the chance of accidentals.

To maximize the coincidence probability, the resonant detectors now in operation are oriented so to be almost parallel each other with an accuracy of 15 degrees. By consequence, a GW burst will produce approximately the same response on every detector of the array, but with shifted time of arrivals.

To state it more rigorously, let A be the amplitude of the GW burst, t_0 the time the wave crosses the origin of the coordinates and $\vec{k}$ the wave unit vector. The time of arrival at the *n*-th site –pointed by the radius vector $\vec{r}_n$– is

$$t_n(\vec{k}, t_0) = t_0 + \vec{k} \cdot \vec{r}_n \qquad (3.12)$$

The amplitude of the detected signal is multiplied by a factor that depends only on $\vec{k}$ through the antenna pattern, which is approximately the same for all the detectors, and therefore the detected amplitude $\hat{A}_{(n)}$ is of the same order of magnitude for all detectors thanks to their quasi-parallel orientation, and depends only slightly on $\vec{k}$.

Therefore, the search patterns for the matched filters differ only for a scale factor that multiplies the amplitude, and a time delay.

Until the existing detectors will carry on independent signal search, each one producing a list of candidate events, event detection will always be in the form of a multiple coincidence. We shall therefore treat first this kind of approach, and then we'll return to a more ideal data processing method.

a) Coincidence-likelihood method

We say we have a *coincidence* between events from different detectors when their times of arrival $\{t_n\}$ lay in the same time window.

If the timing errors are sufficiently small, the set $\{t_n\}$ can be further fitted by (3.12) to give $\vec{k}$ and t_0 (or to reject the coincidence if the data don't fit).

In any case, we are given the set $\{\hat{A}_{(n)}\}$ of *independent* estimates of the amplitude A, and we wish to combine them into the best estimate $\hat{A}_{all}$ satisfying a maximum-likelihood criterion. As the $\hat{A}_{(n)}$ are RGV, with variance $\sigma^2_{\hat{A}_{(n)}}$, it is well known that the solution is the weighted mean

$$\mathbf{A}_{all} = \frac{\sum_{n=1}^{N_d} \frac{\mathbf{A}_{(n)}}{\sigma^2_{\mathbf{A}_{(n)}}}}{\sum_{n=1}^{N_d} \frac{1}{\sigma^2_{\mathbf{A}_{(n)}}}} \qquad (3.13)$$

which is a GRV too, with variance given by

$$\sigma_{\mathbf{A}_{all}} = \left(\sum_{n=1}^{N_d} \sigma^{-2}_{\mathbf{A}_{(n)}}\right)^{-1} . \qquad (3.14)$$

As far as we keep separate the problem of amplitude estimate to that of $\vec{k}$ and t_0, it can be shown that $\mathbf{A}_{all}$ maximize also the overall likelihood function L_{all} of the combined data set from all detectors.

In fact, for the nth detector we recast (1.25) as

$$L_{(n)}\left(\{x_i^{(n)}\}; A\right) \propto \exp\left[-\tfrac{1}{2}\sum_{ij}\mu_{ij}^{(n)}\left(x_j^{(n)} - A\,\mathrm{u}_j^{(n)}\right)\left(x_j^{(n)} - A\,\mathrm{u}_j^{(n)}\right)\right] = \qquad (3.15)$$

$$= \exp\left[-\tfrac{1}{2}\left(\sum_{ij}\mu_{ij}^{(n)}x_i^{(n)}x_j^{(n)} - \frac{\hat{A}^2_{(n)}}{\sigma^2_{\hat{A}_{(n)}}} + \frac{\left(\hat{A}_{(n)} - A\right)^2}{\sigma^2_{\hat{A}_{(n)}}}\right)\right] \equiv \exp\left[-\tfrac{1}{2}\left(\mathrm{X}_{(n)} + \frac{\left(\hat{A}_{(n)} - A\right)^2}{\sigma^2_{\hat{A}_{(n)}}}\right)\right]$$

Where $\mathrm{X}_{(n)}$ is the localized version of the $\mathbf{X}$ test statistics. Then we obtain

$$L_{all} = \prod_{n=1}^{N_d} L_{(n)} \propto \exp\left[-\tfrac{1}{2}\sum_{n=1}^{N_d}\mathrm{X}_{(n)}\right] \cdot \exp\left[-\sum_{n=1}^{N_d}\frac{\left(\hat{A}_{(n)} - A\right)^2}{2\sigma^2_{\hat{A}_{(n)}}}\right] \qquad (3.16)$$

We recognize in the last factor the likelihood function for the set $\{\hat{A}_{(n)}\}$ alone, that is already maximized by the WK filter on each detector. The $\mathrm{X}_{(n)}$ variable doesn't depend on

A, and is supposed to be evaluated independently for the n-th detector using $N_{(n)}$ whitened data samples containing the signal.

This is a remarkable result. On the basis of (3.13) alone we would have used the N_d-1 degrees of freedom χ^2 variable

$$X_{\hat{A}} \equiv \sum_{n=1}^{N_d} \frac{\left(\hat{A}_{(n)}^2 - \hat{A}_{all}^2\right)}{\sigma_{\hat{A}_{(n)}}^2} \qquad (3.17)$$

while now more correctly we define an overall X_{all} for a multiple detection from the value the overall log-likelihood assume at its minimum $\hat{A}_{all}$:

$$X_{all} \equiv \sum_{n=1}^{N_d} X_{(n)} + X_{\hat{A}}\,. \qquad (3.18)$$

This way we have gained a powerful $N_d \cdot (N_{(n)}-1)-1$ degrees of freedom χ^2 test statistic. This will be helpful in the near future when the bandwidth of the detectors is hopefully improving of a factor 10. Then signal duration in the filtered (and whitened data) is going to decrease of the same factor, and so the number of degree of freedoms, unless the frequency span used for χ^2 test is enlarged also (this can be difficult in many respect).

b) "Orthodox" likelihood minimization

In the calculations above, we have left over the implicit dependence of the likelihood function on $\vec{k}$ and t_0, because we considered an array of parallel detectors, and we were interested in maximization only with respect to signal amplitude.

If we want a maximum likelihood estimate of $\vec{k}$ and t_0, and perhaps also of the polarization angle ϕ of the GW (if the detectors are not parallel), a more complex procedure has to be adopted, involving exchange of the raw data, at least sub-sampled in the reduced bandwidth, and a time consuming maximization nonlinear procedure. In practice, we should try to maximize

$$L_{all}\left(\left\{x_i^{(1)}\right\},\left\{x_i^{(2)}\right\},\cdots\left\{x_i^{(N_d)}\right\}; A, t_0, \vec{k}, \phi\right) \propto \prod_n \exp\left[-\tfrac{1}{2}\sum_{ij}\mu_{ij}^{(n)}\left(x_j^{(n)} - A\,u_j^{(n)}(t_0,\vec{k},\phi)\right)\left(x_j^{(n)} - A\,u_j^{(n)}(t_0,\vec{k},\phi)\right)\right] \qquad (3.19)$$

by moving the set $\left\{A, t_0, \vec{k}, \phi\right\}$ in the 5-dimensional space of possible values that these parameters could take.

At the end of the process, the log-likelihood in the minimum furnish a $N_d \cdot N_{(n)}$-5 degrees of freedom test statistic.

As an exercise to probe the efficiency of this χ_{A^2} test we randomly grouped the AURIGA events exchanged under the IGEC in random triplets and quintuplets, and then performed an amplitude consistency check with the method presented above. The result is shown in Table 1. The relatively low fractions of rejected random coincidences are likely a lower limit of the method, because AURIGA showed a stable noise performance in that time period and therefore most of its exchanged events are close to SNR=5 and do have the same amplitude within the proper σ. The efficiency of rejection should increase significantly for higher SNR events and/or in the case that the detectors are not setting the same amplitude thresholds. However, Especially in dealing with high SNR events, care must be taken to account for inaccuracies of the detector calibrations.

Table 1 – **Implementation of χ_A^2 on randomly chosen triplets and quintuplets from AURIGA candidate events.**

Confidence Level	Random triplets Fraction rejected	Random quintuplets Fraction rejected
0.9	0.23	0.30
0.99	0.11	0.17

This goodness-of-the-fit method can be generalized to the case of detectors with different antenna patterns at the cost of solving also for the two parameters describing the source location, unless this is known by other means. It has recently been proposed also a different approach aimed at testing amplitude consistency in 2-fold coincidences between parallel detectors. The approach consists in checking how the value of the logarithm of the ratio of the amplitudes of the events in coincidence compares with the distribution of the values calculated for spurious coincidences, as those generated by time shifting the response of one detector with respect to the other.

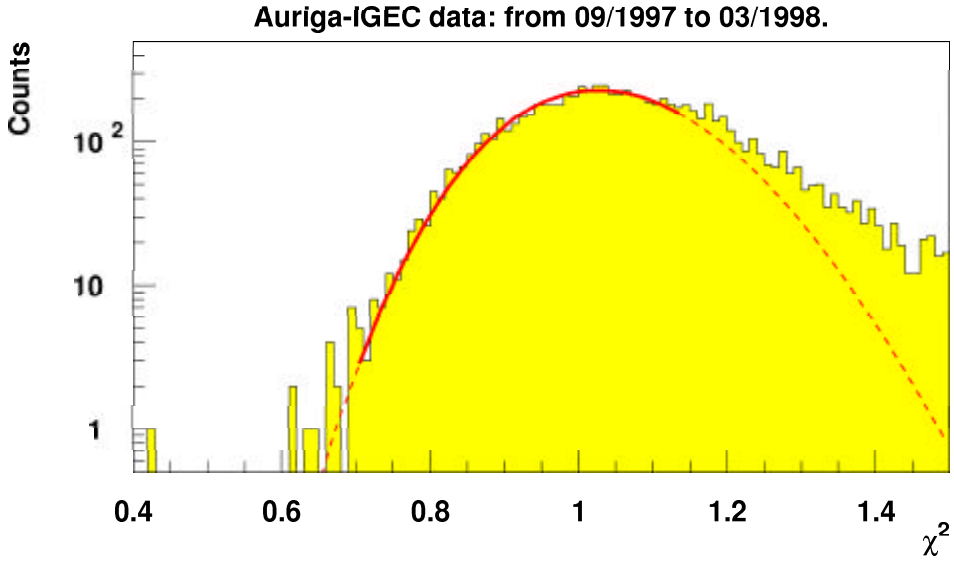

Figure 30. Histogram of the calculated χ_e^2 of the candidate events of the AURIGA detector under the IGEC Collaboration from Sep 1997 to Mar 1998. These 15854 events have been selected by SNR>5 and are below a χ_e^2 threshold which corresponds to a false dismissal of about 1×10^{-4}. The χ_r^2 distribution is also shown as a continuous line.

3.3 *Integrated analysis*

By performing a maximum likelihood analysis on all detectors data the resonant detector observatory behave like a single wide band detector, with noise sources that are uncorrelated between different frequency regions.

3.3.1 Correlation vs. coincidence analysis

Data analysis performed within IGEC is up to now limited to of event information exchanged *after* the event search algorithm, the next step is the investigation of methods for a data analysis using waveforms of the events, or better to perform event search after a multivariate WK filtering applied to the raw data of all detectors.

There are three issues involved with exchanging continuous data streams.

- to make filtering and event search of the same dataset with all different analysis adopted by the four different IGEC groups, for diagnostic purposes, and to highlight any systematic error in the effective temperature estimate, timing, etc.
- to make a correlation analysis instead of simple coincidences analysis; for instance, a weighted average of the filtered data could reduce the variance of the noise, therefore the SNR (and the sensitivity) would be greater.
- to build a common data analysis software, in order to develop a coherent and state-of-the-art analysis joining the efforts of many people involved with data analysis.

An informal discussion is still open about the purposes and the methods of this extended data exchange.

3.3.2 Methods for exchanging continuous data streams between IGEC detectors

Data is acquired from each detector at different sampling rates and saved in different file formats. To remove the need to develop individual processing algorithms for data from each detector, a common data format (cdf) have been proposed to IGEC task force, under which the data is exchanged (see Figure 31) [20]. The cdf will consist in a series of blocks, each one corresponding to a validated time span, within which a continuous data stream is given, along with a header containing a set of mandatory information (e.g. sampling frequency,

Figure 31 – Path of data analysis using the CDF

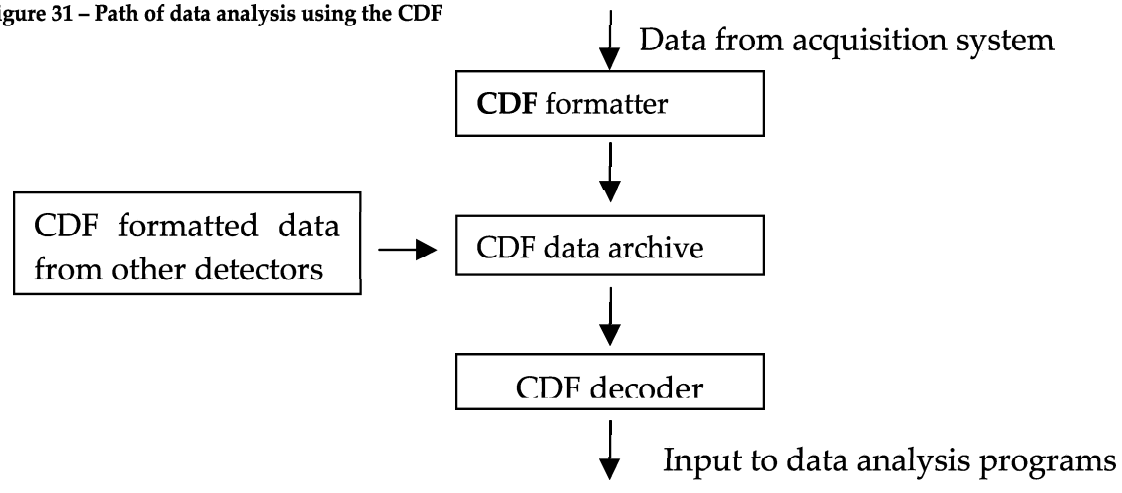

amount of frequency demodulation, etc.).

1. Raw data

EXCHANGED DATA:

Unprocessed data acquired by the data acquisition system of each detector
Transfer function of the system

PRO:

- No need for a new analysis system
- Can be used to examine other phenomena apart from searching from gravitational waves

CON:

- Need to reformat the data according to the analysis of each individual data analysis system
- Need transfer function of the system and calibration information for each detector throughout its operation

2. "True" raw data

EXCHANGED DATA:

Data from the data acquisition system is divided by the transfer function of the detector before being exchanged

PRO:

- Calibrated by each individual group
- All information in one stream of data (eg. in terms of time and amplitude in H_0)
- Can compare signal templates directly to the exchanged data

CON:

- No analysis software ready for this data, need to develop a sophisticate estimator for the noise

3. Filtered data

EXCHANGED DATA:

Data filtered by the Wiener filter developed by each group

PRO:

- No need for calibration or transfer function from each detector (if we do not wish to perform a chi-square test)
- Easy to analyse for different signal templates

CON:

- Cannot check analysis and perform diagnostic tests on the data